Available online at www.sciencedirect.com
SCIENCE DIRECT®
Journal of Organometallic Chemistry 686 (2003) 66–74
Journal of Organometallic Chemistry
www.elsevier.com/locate/jorganchem

Halide induced epimerization of *meso*-1,2-dihalo-1,2-diaryl-1,2-dimethyldisilanes

Kevin A. Trankler, Joyce Y. Corey *, Nigam P. Rath

University of Missouri–St. Louis, St. Louis, MO 63121, USA

Received 10 March 2003; received in revised form 9 May 2003; accepted 9 May 2003

Abstract

Kinetic data were obtained for the halide induced epimerization of *meso*-X[(*p*-RC_6H_4)MeSi]$_2$X (halide = Cl^- where X = F, R = H, CH_3O, CH_3, F, CF_3; halide = Br^- where X = Cl, R = H) to a 1:1 *meso*:*racemic* mixture of diastereomers. A Hammett plot demonstrates a correlation of the rate of epimerization of the fluorinated derivatives with electropositive character at silicon. In order to extend the series of *para*-substituted derivatives, F[(*p*-RC_6H_4)MeSi]$_2$F (R = CF_3) was prepared by treatment of H[(*p*-RC_6H_4)MeSi]$_2$H (R = CF_3) with $CuCl_2$/CuI/KF in THF and the *meso* diastereomer was resolved via crystallization induced asymmetric transformation and the structure verified by X-ray crystallography. Possible mechanisms for the halide induced epimerization are discussed.

Keywords: Disilanes; Halogenation; Epimerization

1. Introduction

Previous investigations on the preparation of fluorine terminated disilanes, F[(*p*-RC_6H_4)MeSi]$_2$F, (R = H, CH_3, CH_3O, F) led to an interesting observation during isolation of the product [1,2]. The 1,2-difluorodisilanes distill as colorless oils containing both diastereomers, *meso* and *racemic*, in a 1:1 ratio. When the distilled oil solidified the resulting solid was found to be enriched in one of the diastereomers. If the distilled oil was crystallized from solvent, the mother liquor remained as a 1:1 ratio of both diastereomers while the crystallized solid contained only a single diastereomer. The isolated single diastereomer in all four cases was the *meso* form as verified by X-ray crystallography. The enhancement of one of the diastereomers during crystallization is consistent with the phenomenon defined as crystallization induced asymmetric transformation (AT) [3]. The occurrence of AT provides access to one diastereomer, usually in high yields ($\geq$90%), from a mixture of diastereomers. Thus, it is possible to obtain reasonable quantities of a diastereomerically pure product to develop further chemistry.

The first stereochemical studies of halogen–halogen exchange at asymmetric silicon centers were performed in the early 1960s, utilizing α-naphthylphenylmethylhalosilanes [4,5]. The monosilanes, R_3Si^*X (R_3 = α-napthyl(Ph)Me), were reacted with ammonium halides resulting in racemization when X = Cl and the incoming halide is Cl, Br, I or exchange at silicon when the incoming halide is F^- and X = Cl or when the incoming halide is Cl^- replacing X = Br. In the cases where exchange products were identified, the exchange was accompanied by inversion of stereochemistry at silicon. In the cases where exchange products were not observed, racemization occurred, although the mechanism was not obvious at the time [6–8].

We have previously reported the fluoride induced epimerization of *meso*-F[(*p*-RC_6H_4)MeSi]$_2$F, (R = H, CH_3, CH_3O, F) and *meso*-Cl(PhMeSi)$_2$Cl [2]. To our knowledge, this was the first example of halide induced epimerization of a diastereomerically pure disilane. In the current report, we will discuss the preparation and isolation of an additional member of the 1,2-difluorodisilane series *meso*-F[(*p*-RC_6H_4)MeSi]$_2$F (R = CF_3) as well as the F^-, and Cl^- induced epimerization of the

* Corresponding author.
E-mail address: corey@umsl.edu (J.Y. Corey).

0022-328X/03/$ - see front matter © 2003 Elsevier Science B.V. All rights reserved.
doi:10.1016/S0022-328X(03)00434-0

meso form and the Cl^-, and Br^- induced epimerization of *meso*-$Cl(PhMeSi)_2Cl$. Kinetic data have been collected and rate constants determined for the Cl^- induced epimerization of *meso*-$F[(p\text{-}RC_6H_4)MeSi]_2F$, (R = H, CH_3, CH_3O, CF_3, F) to generate a Hammett plot. A possible mechanism for the epimerization process will be presented.

2. Results

2.1. Synthesis of dihalides and isolation of meso-X[(p-RC_6H_4)MeSi]$_2$X (X = F, R = H, CH_3, CH_3O, F, CF_3; X = Cl, R = H)

The preparation of $F[(p\text{-}RC_6H_4)MeSi]_2F$ (R = H, CH_3, CH_3O, and F) was reported previously through the treatment of the corresponding hydrosilane, $H[(p\text{-}RC_6H_4)MeSi]_2H$, with $CuCl_2$–CuI–KF in THF in good yields (70–90%) [1,2]. The products were obtained as colorless oils with a 1:1 ratio of *meso* and *racemic* forms. Upon crystallization from appropriate solvents, the occurrence of AT provided single diastereomers. To expand the series of derivatives for kinetic studies the additional 1,2-difluorodisilane with $R = CF_3$ was prepared by the same route (see Section 5). Crystallization from hexanes afforded a single diastereomer of $F[(p\text{-}CF_3C_6H_4)MeSi]_2F$ which was verified as the *meso* form by X-ray crystallography. Selected bond lengths and angles are given in Table 1 and are within the range of those reported previously for the other 1,2-difluorodisilanes. An ORTEP diagram is shown in Fig. 1.

The preparation of $Cl(PhMeSi)_2Cl$ was accomplished in a similar manner by treating $H(PhMeSi)_2H$ with $CuCl_2$/CuI in THF or benzene. The product was obtained as a colorless oil with a 1:1 ratio of diastereomers. Crystallization of $Cl(PhMeSi)_2Cl$ from pentane provided a diastereomerically enriched solid. The enriched diastereomer was the *meso* form as determined by comparison to literature data [9]. Other methods were used for the preparation of $Cl(PhMeSi)_2Cl$ including treatment of $H(PhMeSi)_2H$ with NCS (*N*-chlorosuccinimide) in CCl_4 and treatment of $H(PhMeSi)_2H$ with $SOCl_2$ in CCl_4. Both of these methods also provided the product, however, the yields were reduced when compared to the $CuCl_2$–CuI preparations and the necessity of CCl_4 as a solvent was less desirable.

Table 1
Selected bond lengths (Å) and bond angles (°) in *meso*-$F(p\text{-}CF_3C_6H_4SiMe)_2F$

Bond lengths			
Si–Si	2.3469(9)	Si–C(1) (Me)	1.838(2)
Si–F	1.6039(12)	Si–C(2) (Ar)	1.8688(17)
Bond angles			
F–Si–C(1)	109.22(9)	C(1)–Si–C(2)	112.77(8)
F–Si–C(2)	105.38(7)	C(3)–C(2)–C(7)	117.14(16)
F–Si–Si′	106.08(5)	C(4)–C(5)–C(6)	119.90(17)

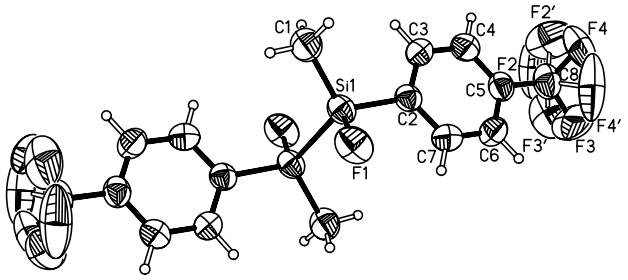

Fig. 1. Projection view of *meso*-$F[(p\text{-}CF_3C_6H_4)MeSi]_2F$ with thermal ellipsoids drawn at 50% probability and showing the rotational disorder in the CF_3 groups.

2.2. Halide induced epimerization of X(ArMeSi)$_2$X

Addition of tetrabutylammonium fluoride, TBAF, (< 10% relative to the disilane) to a $CDCl_3$ solution of *meso*-$F[(p\text{-}RC_6H_4)MeSi]_2F$ resulted in an immediate epimerization of the *meso* forms to a 1:1 mixture of *meso* and *racemic* diastereomers. The rate of epimerization was too rapid to be monitored on the NMR time scale either at ambient temperatures or at −60 °C. Utilization of 'less aggressive' anionic fluoride sources such as $[^nBu_4N][Ph_3SnF_2]$ or Selectfluor, 1-(chloromethyl)-4-fluoro-1,4-diazoniabicyclo[2.2.2]octanebis(tetrafluoroborate), also induced rapid epimerization. At the other extreme, covalent fluoride sources such as Ph_2SiF_2, Me_3SnF, and Ph_3SnF also failed to promote epimerization of the *meso* diastereomer. However, the anionic chloride source, $Bz_2Me_2N^+Cl^-$, promoted epimerization of *meso*-$F[(p\text{-}RC_6H_4)MeSi]_2F$ to a 1:1 mixture of *meso* and *racemic* diastereomers at a sufficiently slow rate (2–3 h) to monitor the process by ^{1}H-NMR spectroscopy. This allowed acquisition of kinetic parameters for the epimerization of *meso*-$F[(p\text{-}RC_6H_4)MeSi]_2F$. Epimerization experiments were carried out by obtaining an initial ^{1}H-NMR spectrum of the disilane in $CDCl_3$ to determine the initial diastereomer ratio by integration of the SiMe region of the spectrum. The anionic chloride source as a solution in $CDCl_3$ was then added and a series of ^{1}H-NMR spectra were collected at timed intervals until the epimerization was complete as observed by a 1:1 diastereomer ratio (~2–3 h).

In a related manner, addition of $Bz_2Me_2N^+Cl^-$ (< 10% relative to the disilane) to a solution enriched in *meso*-$Cl(PhMeSi)_2Cl$ (76:24 *meso*:*racemic*) resulted in immediate epimerization to a 1:1 mixture of *meso* and *racemic* diastereomers. A reduction in the rate of epimerization was observed by using the bromide source $^nBu_4N^+Br^-$ as a catalyst to promote epimerization.

Table 2
Crystal data and structure refinement for *meso*-F(*p*-$CF_3C_6H_4SiMe)_2F$

Empirical formula	$C_{16}H_{14}F_8Si_2$
Formula weight	414.45
Temperature (K)	223(2)
Wavelength (Å)	0.71073
Crystal system	Monoclinic
Space group	*C*2/*c*
Z	4
Unit cell dimensions	
a (Å)	21.5687(2)
b (Å)	5.5963(1)
c (Å)	17.4490(2)
α (°)	90
β (°)	116.275(1)
γ (°)	90
V (Å^3)	1888.58(4)
D_{calc} (Mg m^{-3})	1.458
Absorption coefficient (mm^{-1})	0.259
θ Range for data collection (°)	2.11–26.39
Reflections collected/unique	19679/1911/[$R_{int} = 0.026$]
Goodness-of-fit on F^2	1.031
Final *R* indices [$I > 2\sigma(I)$]	$R_1 = 0.0359$, $wR_2 = 0.0978$
R indices (all data)	$R_1 = 0.0446$, $wR_2 = 0.1036$
Largest difference peak and hole (e Å^{-3})	0.264 and −0.160

2.3. Temperature dependent epimerization of meso-F(PhMeSi)$_2$F

Temperature dependent kinetic data were collected for the $Bz_2Me_2N^+Cl^-$ epimerization of the parent system, *meso*-$F(PhMeSi)_2F$, at 280, 300, 310 and 330 K. The data were collected using ^{1}H-NMR and the relative concentrations of *meso* and *racemic* diastereomers were determined in $CDCl_3$ where resolution of the SiMe diastereomer signals is sufficient to obtain the integration of the two diastereomers. The kinetic data were plotted according to Eq. (1), where x_e is the equilibrium concentration of the *meso* diastereomer and a_0 is the initial concentration of the *meso* diastereomer [10]. This equation takes into account incomplete conversion of starting material to product, which best describes the epimerization of *meso* to a 1:1 mixture of *meso* and *racemic* diastereomers. The data were plotted as log *k* versus 1/*T* to provide the pseudo first-order rate constant for epimerization. The kinetic data are plotted

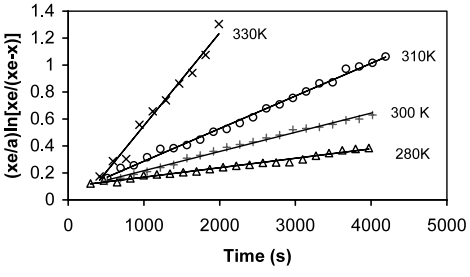

Fig. 2. Temperature dependent rate plots for chloride induced epimerization of *meso*-$F(PhMeSi)_2F$.

Table 3
Temperature dependent rate constants for chloride induced epimerization of *meso*-$F(PhMeSi)_2F$

T (K)	*k* (s^{-1})
280	7.05×10^{-5}
300	1.42×10^{-4}
310	1.98×10^{-4}
330	7.01×10^{-4}

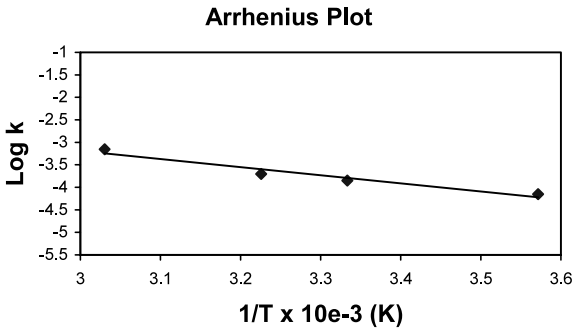

Fig. 3. Arrhenius plot for chloride induced epimerizaiton of *meso*-$F(PhMeSi)_2F$. Linear regression analysis provides a straight line corresponding to the equation $y = -1.80x + 2.21$ with a R^2 value of 0.95.

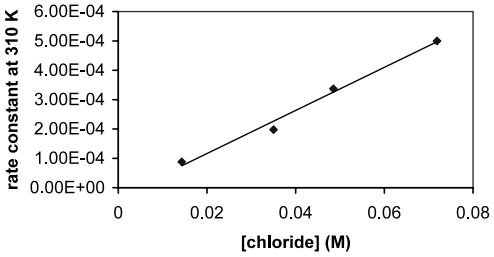

Fig. 4. Chloride dependence plot. Linear regression analysis provides a straight line corresponding to the equation $y = 0.0073x - 3 \times 10^{-5}$ with a R^2 value of 0.98.

for the four different temperatures in Fig. 2 and the resulting rate constants are reported in Table 3. An Arrhenius plot is shown in Fig. 3. The entropy was calculated from the resulting Arrhenius plot as −209 J mol^{-1}.

$$kt = \frac{x_e}{a_0} \ln \frac{x_e}{x_e - x} \quad (1)$$

The chloride dependence was determined by obtaining rate constants at various concentrations of $Bz_2Me_2N^+Cl^-$ at 310 K. The rate constant for the catalyst, k_{cat}, was calculated from the plot of k_1 versus the concentration of $Bz_2Me_2N^+Cl^-$ (see Fig. 4) using the relationship $k_1 = k_{cat}[Bz_2Me_2N^+Cl^-]$ and found to be 7.29×10^{-3}.

3. Discussion

3.1. Halogenation of $H(PhMeSi)_2H$

The first reported preparation of $Cl(PhMeSi)_2Cl$ was accomplished by the treatment of 1,2-dimethyl-1,1,2,2-tetrachlorodisilane with PhMgBr [11]. Attempts to resolve the two diastereomers by crystallization from hexanes were not successful. However, the resolution of the diastereomers by crystallization from pentane was later reported by Sakurai and coworkers resulting in the isolation of a single diastereomer of $Cl(PhMeSi)_2Cl$ which was identified as the *meso* form by X-ray crystallography [9].

We were unable to extend the 1,2-dihalodisilane series to the bromide. Success in bromination of monosilanes has been reported using $CuBr_2$–CuI in a similar manner to the fluorination and chlorination described in the results [12]. The extent of bromination, mono- or dibromination, of R_2SiH_2 can be controlled somewhat by stoichiometry with two equivalents of $CuBr_2$ being required per SiBr formed. The authors successfully brominated one silicon center in the disilane HEt_2Si-$SiEt_2H$, however, dibromination was not attempted, and SiSi bond cleavage was already evident in the products of monobromination. In our attempts to prepare $Br(PhMeSi)_2Br$ we found it was necessary to use benzene as the solvent to suppress undesired side reactions with etherated solvents. Significant Si-Si cleavage products were observed in the product mixture and characterization of the product was difficult due to its sensitivity to moisture. Attempts to characterized the distilled product were not successful due to rapid degradation. The product was derivatized by reaction with MeLi to provide 1,1,2,2-tetramethyl-1,2-diphenyldisilane along with significant amounts of trimethylphenylsilane.

A recent literature method for the preparation of bromosilanes utilized either $PdCl_2$ or $NiCl_2$ as a catalyst and RBr (R = allyl, ethyl, or propyl) as the bromine source [13]. This approach showed increase success in bromination of monosilanes over the $CuBr_2$ route with higher yields (85–95%), but no disilanes were used as substrates.

3.2. Kinetics

Although the fluoride induced epimerization of *meso*-$F(PhMeSi)_2F$ was too rapid to obtain kinetic data, the chloride induced epimerization of *meso*-$F(PhMeSi)_2F$ was sufficiently slow to monitor by NMR spectroscopy. The data showed a rate dependence on temperature that was pseudo first order with respect to the disilane at the catalyst concentrations employed. Fluoride anion (10% relative to the disilane) induced epimerization of *meso*-$Cl(PhMeSi)_2Cl$ rapidly and the presence of the Cl/F exchange product, $F(PhMeSi)_2Cl$, was observed in small amounts ($< 5\%$ relative to initial $Cl(PhMeSi)_2Cl$) by gas chromatography and identified by GCMS. The exchange of Cl for F would give rise to a quaternary ammonium chloride salt which could then also effect epimerization of *meso*-$Cl(PhMeSi)_2Cl$. The chloride induced epimerization of *meso*-$Cl(PhMeSi)_2Cl$ was also very rapid, analogous to fluoride induced epimerization of *meso*-$F(PhMeSi)_2F$, however, the bromide induced epimerization of *meso*-$Cl(PhMeSi)_2Cl$ was slow, analogous to the chloride induced epimerization of *meso*-$F(PhMeSi)_2F$.

Table 4
Rate constants for chloride induced epimerization of *meso*-$F[(p\text{-}RC_6H_4)MeSi]_2F$ (R = CH_3, CH_3O, F, CF_3) at 300 K

R	k (s^{-1})
CH_3	3.41×10^{-5}
CH_3O	1.56×10^{-5}
F	4.28×10^{-4}
CF_3	2.33×10^{-3}

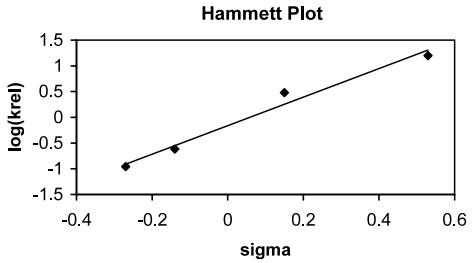

Fig. 5. Hammett plot for chloride induced epimerization of *meso*-$F(ArMeSi)_2F$ (Ar = *p*-$CH_3OC_6H_4$, *p*-$CH_3C_6H_4$, *p*-FC_6H_4, *p*-$CF_3C_6H_4$) at 300 K. Linear regression analysis provides a straight line corresponding to the equation $y = 2.77x - 0.16$ with a R^2 value of 0.98.

The entropy of activation for the chloride induced epimerization of *meso*-$F(PhMeSi)_2F$ is negative and suggestive of a bimolecular process producing a five-coordinate transition state with the disilane and chloride anion participating. Rate constants were also obtained for the chloride induced epimerization of the four other *para*-substituted derivatives of *meso*-$F[(p\text{-}RC_6H_4)MeSi]_2F$ and the values are reported in Table 4. The rate constants were used to generate the Hammett plot shown in Fig. 5. If a bimolecular process was involved in the anionic induced epimerization of the chirotopic silicon center then an increase in the electropositive character at Si* should result in an increase in the rate of epimerization and a Hammett plot should have a positive slope. A plot of the relative rate constants (k_{rel}) versus the literature values for σ (Fig. 5) does, indeed, give rise to a positive slope in agreement with an increase in epimerization rate resulting from an increase in the positive character at Si*.

3.3. Mechanism

The two most obvious mechanistic pathways for anion induced epimerization are (1) substitution with halogen exchange, and (2) formation of a five-coordinate silicate, followed by a series of pseudorotations. The halogen exchange pathway would likely result in the fastest rate of epimerization on the premise of least motion and exchange products would be present by necessity if the attacking halide differs from the silicon bound halide. In the cases of fluoride induced epimerization of *meso*-F(PhMeSi)$_2$F and chloride induced epimerization of *meso*-Cl(PhMeSi)$_2$Cl, the exchange pathway cannot be determined without labeling studies and may be the reason for the more rapid rate of epimerization in those cases compared to the chloride induced epimerization of *meso*-F(PhMeSi)$_2$F and bromide induced epimerization of *meso*-Cl(PhMeSi)$_2$Cl, where slower rates of epimerization were observed. The slow rate of epimerization and lack of detectable exchange products in the Cl^-/F(PhMeSi)$_2$F and Br^-/Cl(PhMeSi)$_2$Cl cases by GC/GCMS suggests that an exchange mechanism is less likely (or absent). Instead, the pseudorotation pathway seems to be supported where the anion attacks at Si* to form a five-coordinate intermediate which then undergoes a series of pseudorotations resulting in inversion at Si* followed by dissociation of the attacking anion and return of Si* to its original four-coordinate state as shown in Fig. 6. The difference between the two pathways for the epimerization of *meso*-X(PhMeSi)$_2$X could be influenced by the size and polarizability of the attacking halide and the relative strengths of the two Si–halogen bonds in the higher coordinate intermediate. When the incoming halide ion is the same as the halogen substituent in the disilane (i.e. F^-/F(PhMeSi)$_2$F and Cl^-/Cl(PhMeSi)$_2$Cl) there would be no difference in silicon–halogen bond strength and either halide could leave the silicon center after epimerization takes place. However, when a larger and more polarizable halide is used (i.e. Cl^-/F(PhMeSi)$_2$F and Br^-/Cl(PhMeSi)$_2$Cl) the attacking halide forms the weaker bond to the silicon center and becomes the preferential leaving group after epimerization has occurred.

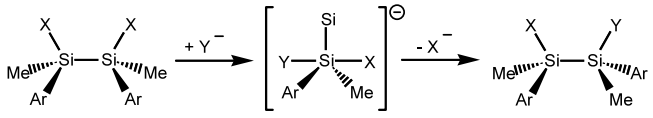

Pathway A, Substitution

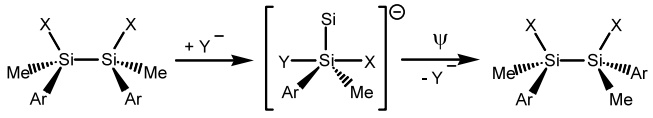

Pathway B, Pseudorotation

Si-X	Y^-	Possible pathway(s)
X = F	F	A and B
	Cl	B only
	Br	B only
X = Cl	F	A and B
	Cl	A and B
	Br	B only

Fig. 6. Possible mechanisms for the halide induced epimerization of *meso*-X(ArMeSi)$_2$X.

4. Conclusion

In the cases where the epimerization of X[(*p*-RC$_6$H$_4$)MeSi]$_2$X is induced by a halide that is the same as or smaller than the halide on silicon, the epimerization process may result from a substitution pathway similar to the S_N2 mechanism described for the monosilanes examined by Sommer et al. [6]. This mechanism, however, does not appear to be responsible for epimerization when the halide is larger than the halide on silicon, such as the Cl^- induced epimerization of *meso*-F(ArMeSi)$_2$F. In these cases, no substitution products were detected and an alternative mechanism was required to account for the results and the formation of a five-coordinate intermediate that then undergoes pseudorotation followed by loss of the incoming halide resulting in the inversion of stereochemistry was proposed. The kinetic data obtained supported a mechanism involving a bimolecular process such as the S_N2 substitution pathway or the pseudorotation pathway suggested in both cases. It has not been determined at this point whether epimerization is unique to 1,2-dihalodisilanes or if other functional groups such as 1,2-diaminodisilanes or 1,2-dialkoxydisilanes might also undergo epimerization when treated with catalytic amounts of halide anions or other anionic nucleophiles.

5. Experimental

5.1. General considerations

All reactions were performed in flame-dried glassware under dry nitrogen on a dual-manifold Schlenk line. The solvents THF and Et_2O were distilled from Na–benzophenone or Na–9-fluorenone [14] and CH_2Cl_2 was distilled over CaH_2 prior to use. The following reagents were used as supplied commercially: $SOCl_2$, NCS (*N*-chlorosuccinimide), CCl_4, $CuCl_2$, $CuBr_2$, CuI, KF, Cp_2TiCl_2, ^{n}BuLi, $BrC_6H_4CF_3$, Mg, TBAF,

$Bz_2Me_2N^+Cl^-$, and $^nBu_4N^+Br^-$; commercial HOTf was distilled before use. The following reagents were prepared by literature methods: $F(PhMeSi)_2F$ [1], $F[(p\text{-}RC_6H_4)MeSi]_2F$ (R = CH_3, CH_3O, and F) [2], and $H(PhMeSi)_2H$ [15].

Low resolution mass spectral data (EI, 70 eV) were collected on a Hewlett-Packard model 5988A instrument. Gas chromatographic analyses were performed on a Shimadzu model GC-14A gas chromatograph utilizing a 12 m DB-5 capillary column. Proton, $^{13}C\{^1H\}$, and $^{29}Si\{^1H\}$ nuclear magnetic resonance spectra were recorded using either a Varian Unity *plus* 300 equipped with a tuneable broadband probe or a Bruker ARX-500 equipped with a broadband or inverse probe. Spectra are referenced internally to residual solvent peaks ($CHCl_3$ or C_6H_6) or to TMS. ^{19}F-NMR data were collected on an Avance 300 with a multiple nucleus probe using $CFCl_3$ or C_6F_6 as an external reference or on the Bruker ARX-500. Spectra were recorded at r.t. unless specified otherwise, the chemical shifts of the centers of multiplets are listed and coupling constants are given in Hz. The dept sequence was utilized in collecting ^{29}Si-NMR data.

Unless specified otherwise, Kugelrohr distillations were used to purifiy liquid samples. Melting points are uncorrected and were obtained on either a Hoover capillary apparatus (oil bath) or an Electrothermal Engineering Ltd. Digital melting point apparatus series IA9100. Analyses were performed by Atlantic Microlab, Inc.

5.2. $H(p\text{-}CF_3C_6H_4SiMe)_2H$

$H(PhMeSi)_2H$ (5.00 g, 20.7 mmol) was added to 30 ml of CH_2Cl_2, and the solution was cooled to −23 °C (CCl_4, dry ice bath). HOTf (4.00 ml, 45.0 mmol) was then added by syringe with vigorous stirring, resulting in a pale yellow solution. After warming to room temperature (r.t.) the mixture was stirred an additional 45 min. The Grignard reagent was prepared separately by slow addition of $BrC_6H_4CF_3$ (7.00 ml, 50.0 mmol) to Mg (1.34 g, 55.0 mmol) in 120 ml of Et_2O followed by reflux for 1.5 h. The Grignard reagent was added dropwise to the silyl triflate cooled to 0 °C, stirred for an additional hour at 0 °C and then allowed to stand overnight at r.t. Deionized water (200 ml) was added along with saturated NH_4Cl to quench the mixture. The Et_2O layer was separated and the aqueous layer was extracted with portions of Et_2O. The combined organic layers were dried over anhydrous sodium sulfate. The volatiles were removed in vacuo resulting in a pale yellow oil which was distilled to give $H(p\text{-}CF_3C_6H_4SiMe)_2H$ (b.p. 65–80 °C/0.05 mmHg; 6.58 g, 84.0%) as a colorless oil. ^1H-NMR (500 MHz, $CDCl_3$): δ 0.49 (d, $SiCH_3$), 4.48 (m, SiH), 7.57 (m, ArH). ^{19}F-NMR (470 MHz, $CDCl_3$): δ −63.50. $^{29}Si\{^1H\}$-NMR (99 MHz, $CDCl_3$): δ −35.89, −36.12. The disilane was used without further purification for the fluorination step.

5.3. $F(p\text{-}CF_3C_6H_4SiMe)_2F$

A mixture of $CuCl_2$ (3.00 g, 22.3 mmol), CuI (50.4 mg, 0.27 mmol), and KF (0.77 g, 13.2 mmol) was added to a round-bottom flask containing a stir bar. The solid mixture was heated to 100 °C in an oil bath under vacuum (0.1 mmHg) for 12 h. Freshly distilled THF (50 ml) was added after the apparatus cooled to r.t. A rust-orange slurry was formed which was stirred for 15 min. Next, $H(p\text{-}CF_3C_6H_4SiMe)_2H$ (2.00 g, 5.29 mmol) was added by syringe with stirring and the mixture was allowed to react at r.t. After 4 h the starting material had been consumed and the mixture was added to hexanes and filtered through Celite to remove solid material from the clear yellow liquid. The volatiles were removed in vacuo resulting in a pale yellow oil which was purified by distillation to give $F(p\text{-}CF_3C_6H_4SiMe)_2F$ (b.p. 90–115 °C/0.05 mmHg; 1.95 g, 89%) as a colorless oil. The oil contained both diastereomers in an approximate 1:1 ratio by GC (46:54 relative GC integrations). The oil was dissolved in a minimal amount of hexanes and allowed to slowly crystallize at r.t. to give one diastereomer by GC as a white solid (m.p. 60–61 °C, 1.45 g) while the mother liquor contained both diastereomers in an approximate 1:1 ratio (44:56 by GC). Characterization data were obtained on the single diastereomer. ^1H-NMR (300 MHz, C_6D_6): δ 0.28 (A_3B_3XY, $SiCH_3$), 7.27 (d, CH), 7.28 (d, CH). $^1H\{^{19}F\}$ (300 MHz, C_6D_6): δ 0.28 (s, $SiCH_3$), 7.27 (d, CH), 7.28 (d, CH). $^{13}C\{^1H\}$-NMR (75 MHz, C_6D_6): δ −0.90, 125.5, 128.1, 128.4, 128.7, 133.0. ^{19}F-NMR (282 MHz, C_6D_6): δ −181.8 (m, SiF), −63.4 (s, CF_3). $^{19}F\{^1H\}$-NMR (282 MHz, C_6D_6): δ −181.8 (s), −63.4 (s). $^{29}Si\{^1H\}$-NMR (99 MHz, C_6D_6): δ 14.68 (dd, $^1J_{SiF} = 309$ Hz, $^2J_{SiF} = 35$ Hz). Mass spectrum (*m/e* (relative intensities)): 395 ($\{P-F\}^{\bullet+}$, 1), 333 ($Me(p\text{-}CF_3C_6H_4)_2Si^+$, 24), 207 ($FMe(p\text{-}CF_3C_6H_4)Si^+$, 100), 188 ($Me(p\text{-}CF_3C_6H_4)Si^+$, 63), 173 ($p\text{-}CF_3C_6H_4Si^+$, 32). Anal. Calc. for $C_{16}H_{14}Si_2F_8$: C, 46.37; H, 3.41. Found: C, 46.76; H, 3.41.

5.4. $Cl(PhMeSi)_2Cl$ via $CuCl_2/CuI$

A flame dried apparatus was charged with $CuCl_2$ (7.33 g, 54.6 mmol) and CuI (120 mg, 0.62 mmol). The solid mixture was heated to 100 °C in an oil bath under vacuum (0.1 mmHg) for approximately 12 h. Freshly distilled Et_2O (80 ml) was added by syringe after the apparatus had cooled to r.t. The mixture was allowed to stir at r.t. for approximately 15 min followed by the addition of $H(PhMeSi)_2H$ (3.00 g, 12.4 mmol) by syringe with stirring. The progress of the reaction was monitored by withdrawal of aliquots which were treated

with MeLi and analyzed by GCMS. After 5 days, the starting material had been consumed and the reaction mixture was filtered under nitrogen to remove solid material. The volatiles were removed in vacuo resulting in a pale yellow oil which was purified by distillation to give $Cl(PhMeSi)_2Cl$ (b.p. 105–120 °C/0.05 mmHg; 3.19g, 83%) as a colorless oil containing both *meso* and *racemic* diastereomers in a 1:1 ratio from integration of the SiMe signal in the ^{1}H-NMR spectrum. The oil was dissolved in pentane and placed in a −52 °C freezer resulting in the formation of a white crystalline solid which was enriched in the *meso* diastereomer revealed by the ^{1}H-NMR spectrum (76:24). ^{1}H-NMR (500 MHz, $CDCl_3$): δ 0.79 (*meso*, s, 1.00, $SiCH_3$) 0.86 (*racemic*, s, 0.32, $SiCH_3$), 7.35–7.65 (m, Ar*H*). ^{29}Si{^{1}H}-NMR (99 MHz, $CDCl_3$): δ 6.32, 6.42. Published NMR data for *meso*-$Cl(PhMeSi)_2Cl$ [6]: ^{1}H-NMR ($CDCl_3$): δ 0.80 (s, 6H), 7.38–7.47 (m, 6H), 7.59–7.63 (m, 4H). ^{29}Si{^{1}H}-NMR ($CDCl_3$): δ 6.31.

5.5. *Cl(PhMeSi)$_2$Cl via NCS/CCl$_4$*

A flame dried flask equipped with a condenser and stir bar was charged with NCS (2.20 g, 16.5 mmol) followed by the addition of CCl_4 (20 ml). $H(PhMeSi)_2H$ (1.00 g, 4.13 mmol) was added by syringe and the mixture was brought to reflux with stirring. The white slurry was allowed to react at reflux until starting material, $H(PhMeSi)_2H$, was no longer observed by GC (6 days). The reaction mixture was filtered through Celite to remove solid material and the solvent was removed in vacuo to give a pale yellow oil which was purified by distillation to give a colorless oil (b.p. 110–130 °C/0.1 mmHg; 0.90g, 70%). Characterization data were identical to that obtained from the $CuCl_2$–CuI preparation.

5.6. *Cl(PhMeSi)$_2$Cl via SOCl$_2$/CCl$_4$*

To a flame dried flask equipped with a stir bar and condenser containing $H(PhMeSi)_2H$ (1.00 g, 4.13 mmol) and CCl_4 (15 ml) was added $SOCl_2$ (3.00 ml, 41.1 mmol) with stirring. The reaction mixture was brought to reflux and allowed to react with stirring until starting material, $H(PhMeSi)_2H$, was no longer observed by GC (3 days). A small amount of white insoluble material was present which was removed by filtration and washed with CH_2Cl_2. The volatiles were removed in vacuo resulting in a yellow oil which was purified by distillation to give a colorless oil (b.p. 110–125 °C/0.1 mmHg; 0.67g, 53%). Characterization data were identical to that obtained from the $CuCl_2$–CuI preparation.

5.7. *Br(PhMeSi)$_2$Br*

A flame dried flask equipped with a stir bar and condenser was charged with $CuBr_2$ (4.06 g, 18.0 mmol) and CuI (39.0 mg, 0.21 mmol). The solid components were dried under vacuum for 12 h. Freshly distilled benzene (30 ml) was added by syringe and the brown slurry was allowed to stir for approximately 10 min. $H(PhMeSi)_2H$ (1.00 g, 4.13 mmol) was then added by syringe with stirring. After 7 days, the mixture appeared as a golden brown slurry and no disilane, $H(PhMeSi)_2H$, was observed by GC. Solid material was removed by filtration under nitrogen through a Celite column giving a pale yellow liquid. The volatiles were removed in vacuo resulting in a pale yellow oil. This was distilled under nitrogen to give a colorless oil (b.p. 130–145 °C/0.1 mmHg; 0.71 g, 43%) which became golden a brown solid upon standing under nitrogen after 1 day. Treatment of the oil with MeLi resulted in the formation of 1,1,2,2-tetramethyl-1,2-diphenyldisilane (67% by GC) as revealed by GCMS ($M^{+\bullet} = 270$). ^{1}H-NMR for $Br(PhMeSi)_2Br$ (mixture of diastereomers) (300 MHz, C_6D_6): δ 0.83, 0.76 (s, $SiCH_3$), 7.09 (m, Ar*H*), 7.47 (m, Ar*H*), 7.64 (m, Ar*H*). NMR data for 1,1,2,2-tetramethyl-1,2-diphenyldisilane: ^{1}H-NMR (500 MHZ, $CDCl_3$): δ 0.32 (s, $SiCH_3$), 7.29 (m, Ar*H*), 7.37 (m, Ar*H*). ^{29}Si{^{1}H}-NMR (99 MHz, $CDCl_3$): δ −21.8 (s).

5.8. *Catalyzed epimerization of meso-F[(p-RC$_6$H$_4$)MeSi]$_2$F (R = H, CH$_3$, CH$_3$O, F, and CF$_3$)*

R = H. A sample of *meso*-$F[(p\text{-}RC_6H_4)MeSi]_2F$ (24 mg, 8.6×10^{-2} mmol) was dissolved in $CDCl_3$ and a $CDCl_3$ solution of $Bz_2Me_2N^+Cl^-$ (4.5 mg, 20 mol% relative to the disilane) was added. The epimerization was followed by ^{1}H-NMR until a 1:1 ratio of diastereomers was obtained. The data were collected at probe temperatures of 280, 300, 310, and 330 K.

R = CH_3O. A sample of *meso*-$F[(p\text{-}RC_6H_4)MeSi]_2F$ (23 mg, 6.8×10^{-2} mmol) was dissolved in $CDCl_3$ and a $CDCl_3$ solution of $Bz_2Me_2N^+Cl^-$ (3.6 mg, 20 mol% relative to the disilane) was added. The epimerization was followed by ^{1}H-NMR at 300 K until a 1:1 ratio of diastereomers was obtained.

R = CH_3. A sample of *meso*-$F[(p\text{-}RC_6H_4)MeSi]_2F$ (18 mg, 5.9×10^{-2} mmol) was dissolved in $CDCl_3$ and a $CDCl_3$ solution of $Bz_2Me_2N^+Cl^-$ (3.1 mg, 20 mol% relative to the disilane) was added. The epimerization was followed by ^{1}H-NMR at 300 K until a 1:1 ratio of diastereomers was obtained.

R = F. A sample of *meso*-$F[(p\text{-}RC_6H_4)MeSi]_2F$ (20 mg, 6.4×10^{-2} mmol) was dissolved in $CDCl_3$ and a $CDCl_3$ solution of $Bz_2Me_2N^+Cl^-$ (3.3 mg, 20 mol% relative to the disilane) was added. The epimerization was followed by ^{1}H-NMR at 300 K until a 1:1 ratio of diastereomers was obtained.

R = CF_3. A sample of *meso*-F[(*p*-RC_6H_4)MeSi]$_2$F (21 mg, 5.1×10^{-2} mmol) was dissolved in $CDCl_3$ and a $CDCl_3$ solution of $Bz_2Me_2N^+Cl^-$ (2.7 mg, 20 mol% relative to the disilane) was added. The epimerization was followed by ^{1}H-NMR at 300 K until a 1:1 ratio of diastereomers was obtained.

5.9. Chloride dependence

4 different samples of *meso*-F(PhMeSi)$_2$F (25 mg, 9.0×10^{-2} mmol) were dissolved in $CDCl_3$. Sufficient amounts of a $CDCl_3$ solution of $Bz_2Me_2N^+Cl^-$ was added to bring the concentration of $Bz_2Me_2N^+Cl^-$ to 14.3, 35.0, 48.5 and 72.0 mM and $CDCl_3$ was added to bring the total volume to 500 μl. The epimerization was followed by ^{1}H-NMR at 310 K until a 1:1 ratio of diastereomers was obtained.

5.10. Catalyzed epimerization of meso-Cl(PhMeSi)$_2$Cl

5.10.1. TBAF

A sample of Cl(PhMeSi)$_2$Cl (27 mg, 8.7×10^{-2} mmol; *meso*:*racemic* = 76:24) was dissolved in $CDCl_3$ and the ^{1}H-NMR spectrum was obtained. A solution of TBAF (1 M, 4.4 μl; 5 mol% relative to the disilane) was injected and the ^{1}H-NMR spectrum taken immediately. A 1:1 ratio of diastereomers was observed. GCMS analysis also revealed trace amounts (< 5%) of F(PhMeSi)$_2$Cl present in the reaction mixture.

5.10.2. $Bz_2Me_2N^+Cl^-$

A sample of *meso*-Cl(PhMeSi)$_2$Cl (22 mg, 7.1×10^{-2} mmol) was dissolved in $CDCl_3$ and the ^{1}H-NMR spectrum was obtained. A solution of $Bz_2Me_2N^+Cl^-$ (1.9 mg, 10 mol% relative to the disilane) in $CDCl_3$ was added and the ^{1}H-NMR spectrum taken immediately. A 1:1 ratio of diastereomers was observed.

5.10.3. $^nBu_4N^+Br^-$

A sample of *meso*-Cl(PhMeSi)$_2$Cl (26 mg, 8.4×10^{-2} mmol) was dissolved in $CDCl_3$ and a $CDCl_3$ solution of $^nBu_4N^+Br^-$ (5.4 mg, 20 mol% relative to the disilane) was added. The epimerization was followed by ^{1}H-NMR at 300 K until a 1:1 ratio of diastereomers was obtained.

5.11. X-ray crystallography

A single crystal with dimensions $0.33 \times 0.28 \times 0.22$ mm^3 was mounted on a glass fiber in random orientation. Preliminary examination and data collection were performed using a Bruker SMART charge coupled device (CCD) detector single crystal X-ray diffractometer using graphite monochromated Mo–K_α radiation (λ = 0.71073 Å) equipped with a sealed tube X-ray source. Preliminary unit cell constants were determined with a set of 45 narrow frames (0.3° in ϖ) scans. Data collection consisted of 3636 frames of intensity data collected with a frame width of 0.3° in ϖ and counting time of 15 s/frame at a crystal to detector distance of 4.950 cm. The double pass method of scanning was used to exclude any noise. The collected frames were integrated using an orientation matrix determined from the narrow frame scans. SMART and SAINT software packages [16] were used for data collection and data integration. Analysis of the integrated data did not show any decay. Final cell constants were determined by global refinement of *xyz* centroids of 7720 reflections from the complete data set. Collected data were corrected for systematic errors using SADABS [17] based on the Laue symmetry using equivalent reflections.

Structure solution and refinement were carried out using the SHELXTL-PLUS software package [18]. The structure was solved by direct methods and refined successfully in the monoclinic space group *C*2/*c*. Full-matrix least-squares refinement was carried out by minimizing $\Sigma w(F_o^2 - F_c^2)^2$. The non-hydrogen atoms were refined anisotropically to convergence with final residual values: $R_1 = 3.6\%$, $wR_2 = 10.4\%$. The hydrogen atoms were treated using appropriate riding model (AFIX m3). The CF_3 group shows rotational disorder. The disorder was resolved by using two sets of *F* values with partial occupancies. Crystal data and the final structure refinement parameters are listed in Table 2.

6. Supplementary material

Crystallographic data for the structural analysis have been deposited with the Cambridge Crystallographic Data Centre, CCDC no. 204286 for *meso*-F(*p*-$CF_3C_6H_4SiMe)_2F$. Copies of this information may be obtained free of charge from The Director, CCDC, 12 Union Road, Cambridge CB2 1EZ, UK (Fax: +44-1223-336033; e-mail: deposit@ccdc.cam.ac.uk or www: http://www.ccdc.cam.ac.uk).

Acknowledgements

The NSF (grant nos. CHE-9318696 and CHE-9974801) and the University of Missouri Research Board are gratefully acknowledged for support of the purchase of both a Varian Unity Plus 300 spectrometer and a Bruker Avance 300 spectrometer. The UM-St. Louis X-ray Crystallography Facility was funded in part by a NSF Instrumentation Grant (grant no. CHE-9309690) and a UM-St. Louis Research award. Purchase of the mass spectrometer, JEOL Mstation JMS700, was supported by NSF grant no. CHE-9708640. We also thank Peter Gaspar, Janet Brad-

dock-Wilking, and James Chickos for helpful discussions.

References

[1] K.A. Trankler, D.S. Wyman, J.Y. Corey, E.E. Katz, Organometallics 19 (2000) 2408.
[2] K.A. Trankler, D.S. Wyman, J.Y. Corey, E.E. Katz, N.P. Rath, Organometallics 20 (2001) 5139.
[3] (a) J. Jacques, A. Collet, S.H. Wilen, Enantiomers, Racemates, and Resolutions, Krieger Publishing, Malabar, FL, 1994;
(b) M.M. Harris, Prog. Stereochem. 2 (1958) 157;
(c) R.M. Secor, Chem. Rev. 63 (1963) 297.
[4] L.H. Sommer, P.G. Rodewald, G.A. Parker, Tetrahedron 18 (1962) 815.
[5] L.H. Sommer, K.W. Michael, W.D. Korte, J. Am. Chem. Soc. 85 (1963) 3712.
[6] L.H. Sommer, F.O. Stark, K.W. Michael, J. Am. Chem. Soc. 86 (1964) 5683.
[7] L.H. Sommer, D.L. Bauman, J. Am. Chem. Soc. 91 (1969) 7045.
[8] (a) A. Bassindale, Reaction mechanisms of nucleophilic attackat silicon, in: S. Patai, Z. Rappoport (Eds.), The Chemistry of Organic Silicon Compounds, Part 1, Ch. 13, Wiley–Interscience, New York, 1989;
(b) A.R. Bassindale, S.J. Clynn, P.G. Taylor, Reaction mechanisms of nucleophilic attack at silicon, in: Z. Rappoport, Y. Apeloig (Eds.), The Chemistry of Organic Silicon Compounds, Ch. 9, Wiley, Chichester, 1998, pp. 495–511;
(c) D. Kost, I. Kalikham, Hypervalent silicon compounds, in: Z. Rappoport, Y. Apeloig (Eds.), The Chemistry of Organic Silicon Compounds, Ch. 23, Wiley, Chichester, 1998, pp. 1339–1445;
(d) R.J. Corriu, C. Guerin, J.J.E. Moreau, Top. Stereochem. 15 (1984) 43;
(e) L.H. Sommer, Stereochemistry, Mechanism and Silicon, McGraw-Hill, New York, 1965;
(f) R.J.P. Corriu, M. Henner, J. Organomet. Chem. 74 (1981) 1.
[9] A. Sekiguchi, I. Maruki, H. Sakurai, J. Am. Chem. Soc. 115 (1993) 11460.
[10] K.J. Laidler, Chemical Kinetics, 2nd ed., McGraw-Hill, New York, 1965.
[11] K. Tamao, M. Kumada, M. Ishikawa, J. Organomet. Chem 31 (1971) 17.
[12] A. Kunai, T. Ochi, A. Iwata, J. Ohshita, Chem. Lett. (2001) 1228.
[13] A. Iwata, Y. Toyoshima, T. Hayashida, T. Ochi, A. Kunai, J. Ohshita, J. Organomet. Chem. 667 (2003) 90.
[14] M. Kamaura, J. Inanaga, Tetrahedron Lett. 40 (1999) 7347.
[15] J.Y. Corey, X.-H. Zhu, T.C. Bedard, L.D. Lange, Organometallics 10 (1991) 924.
[16] Bruker Analytical X-ray, Madison, WI, 2001.
[17] R.H. Blessing, Acta Crystallogr. Sect. A. 51 (1995) 33–38.
[18] G.M. Sheldrick, Bruker Analytical X-ray Division, Madison, WI, 2001.